15 Apr 2004, 1:00pm - 2:45pm

Expreriment of Seismic Failure of a Long Embankment

Seiji Kano
Hiroshima University, Higashi-Hiroshima, Hiroshima, Japan

Yasushi Sasaki
Hiroshima University, Higashi-Hiroshima, Hiroshima, Japan

Yoshiya Hata
Hiroshima University, Higashi-Hiroshima, Hiroshima, Japan

Proceedings: Fifth International Conference on Case Histories in Geotechnical Engineering
New York, NY, April 13-17, 2004

EXPRERIMENT OF SEISMIC FAILURE OF A LONG EMBANKMENT

Seiji Kano
Hiroshima University
Higashi-Hiroshima, Hiroshima
JAPAN, 7398527

Yasushi Sasaki
Hiroshima University
Higashi-Hiroshima, Hiroshima
JAPAN, 7398527

Yoshiya Hata
Hiroshima University
Higashi-Hiroshima, Hiroshima
JAPAN, 7398527

ABSTRACT

Seismic damage to long structures such as river dikes, fill-type dams, and road embankments has been sometimes found to take place at locally limited spot. Local failures of a long embankment during an earthquake are mainly due to heterogeneous ground condition. However there are some cases that local failures were took place even though the ground condition was homogeneous. One of the factors causing local failures under such conditions may be the three dimensional response of the embankment. In this paper, the typical failure of the Kushiro River dike is reported. This paper aims to clarify the influence of three-dimensional response to local failure in embankments. A series of shaking table tests was carried out. The results reveal that local failure can be caused by periodical three dimensional effects during shaking.

DAMAGE OF THE KUSHIRO RIVER DIKE DURING THE KUISHIRO-OKI EARTHQUAKE IN 1993

Seismic damage to long structures such as river dikes, fill-type dams, and road embankments has been sometimes found to take place at locally limited spot even thought the seismic condition, the geometrical condition of embankment and the foundation condition are the same along their longitudinal direction.
A typical example of this type of damage was seen at the Kushiro River dike during the Kushiro-Oki Earthquake (Mj=7.3) in 1993. Kushiro city is located in the eastern part of Hokkaido, Japan. The Kushiro River runs through the western part of Kushiro city, called the Kushiro bog. A section of the Kushiro River dike, which is 2300 m in length and about 6.2 m in height, had been constructed on flat soft deposit by using sandy materials. The foundation ground was covered by peat layer on the surface underlain by sandy deposit and clay layer and these layers spread almost horizontally. The cross-section of the dike before and after

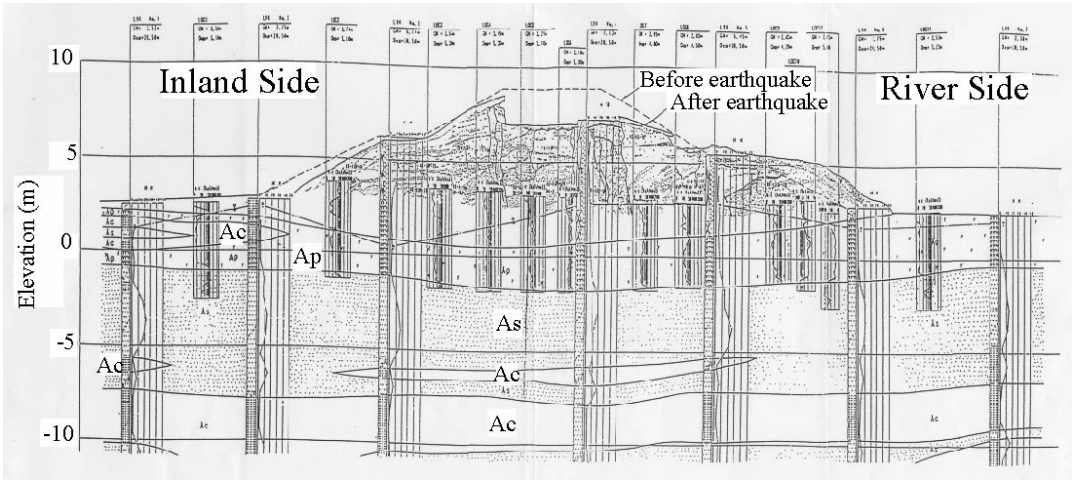

Fig. 1. The Cross-section of the Kushiro River dike at 9.850 KP

Fig. 2. Aerial photograph of the damaged dike

the earthquake is shown in Fig. 1.
This section of the dike suffered to serious damage during the Kushiro-Oki Earthquake. Figure 2 shows an aerial photograph of the damaged section.
According to an in-situ investigation after the earthquake, the maximum subsidence of the crest reached to about 2 m at several spots, accompanied by deep longitudinal fissures at the crest as shown in Fig. 3. The fissures were reported to be about 2 m in width. The lengths of the seriously failed section were about 200-300 m and they appeared periodically along the dike axis.

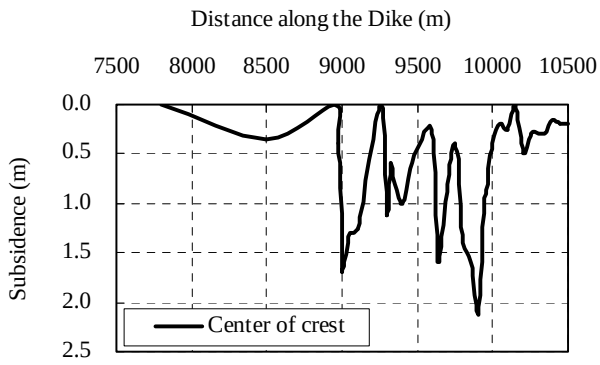

Fig. 3. Subsidence of the Kushiro River dike

Figure 4 shows the Fourier transform of the settlement. The spatially distributed failures of this dike section were found

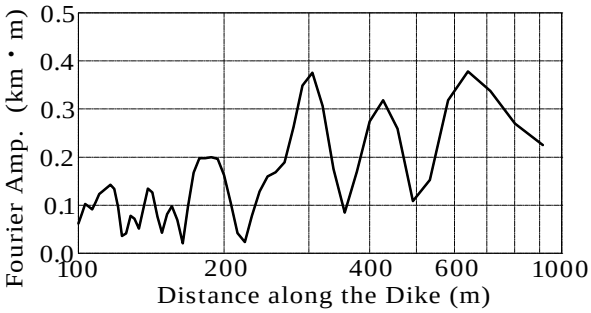

Fig. 4. Fourier spectrum of subsidence of the Kushiro River dike

.

between the failures and were separated by intervals of 300 m.
One can assume several reasons why local failures to a long structure like this occur. One of them is the locally amplified seismic motion due to the three-dimensional behavior of the embankment.
This paper aims to clarify the three-dimensional behavior of an embankment, and to clarify its local failure during an earthquake. A series of model tests was carried out by using small shaking table.

SHAKING TABLE TESTS

Condition of tests

Tests utilizing an electromagnetic shaking table (510 x 510 mm) were carried out. The dynamic response of the top crest was recorded with a high-speed CCD camera. The displacement of the model embankment was measured by using an image analysis system. A Photographable area depends on the size of CCD and its distance to the object; in these tests it was about 130 x 70 mm.
Displacement at the high frequency becomes small. Also it becomes difficult to measure displacement at high frequency by this method if constant acceleration is input. Therefore, in these tests displacement of vibration was kept constant to 1.0mm. Assuming that material properties of a specimen are linear, the displacement observable at the crest could be normalized with the frequency after the tests. X_{10} is defined as the displacement of model embankment under 10 Hz (f_{10}) shaking, and X_A is also defined as that under A Hz. As far as material properties of specimen are linear, the displacement under the same acceleration to the f_{10} vibration is calculated as follows:

$$X = X_A \times \left(\frac{f_{10}}{f_A} \right)^2 . \quad (1)$$

The model embankment was made from milk and gelatin. It has the shape of a triangular prism. The length of the model

embankment was 480 mm and its height was about 40 mm in Series 1 and 2. In Series 1, the slope of the embankment, $H:B/2$, was varied from 1:0.59 to 1:2.3. H is the height of dike and B is the width at embankment base. In Series 2, the shear modulus of model dike was varied from 10440 N/m^2 to 67060 N/m^2. In Series3, the length was varied from 120 mm to 480 mm. Table 1 shows the test condition of each test.

Table 1. Condition of shaking table tests

Case No	H (mm)	B (mm)	H:B/2	L (mm)	Shear modulus (N/m^2)
Series 1-1	33.9	159.5	1:2.35	480	19910
Series 1-2	42.1	164.0	1:1.95	480	19910
Series 1-3	42.8	80.5	1:0.94	480	19910
Series 1-4	45.5	53.2	1:0.59	480	19910
Series 2-1	39.8	83.0	1:1.04	480	10440
Series 2-2	39.7	78.3	1:0.99	480	19910
Series 2-3	41.0	82.4	1:1.01	480	36920
Series 2-4	41.0	87.3	1:1.06	480	56410
Series 2-5	41.0	84.7	1:1.03	480	67070
Series 3-1	41.4	76.9	1:0.93	120	19910
Series 3-2	41.4	76.9	1:0.94	240	19910
Series 3-3	40.5	79.9	1:0.99	360	19910

Wave which appears at a crest of a dike

Figure 5 shows the photograph of model embankment which was taken from above it during the shaking of Series 1-3. It was found that the displacement becomes larger at the locally limited spot. Its amplitude changed periodically along the longitudinal direction like a wave, though model base was shaken parallel with the crest. Consequently, the distribution of cyclic response at the crest of embankment is considered like a harmonic wave, and the wavelength l of this harmonic wave can be calculated using the Fast Fourier Transfer (FFT). As shown in Fig. 6, Y is defined as a longitudinal axis of embankment and X is defined as the orthogonal axis cross to dike. $X_{\max}$ and $X_{\min}$ are defined as the extreme values of amplitude of wave. An amplitude at the anti-nodal point $X_{Antinode}$ is defined as the greater of $X_{\max}$ and $X_{\min}$. The amplitude at a nodal point, X_{Node} is defined as halfway point between $X_{\max}$ and $X_{\min}$. So a half–amplitude of the wave is defined as $X_{Antinode} - X_{Node}$.

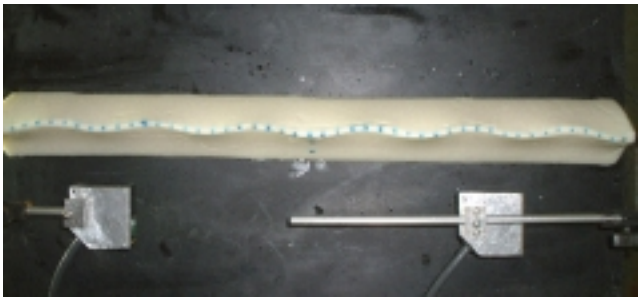

Fig.5. Photograph of embankment during the shaking

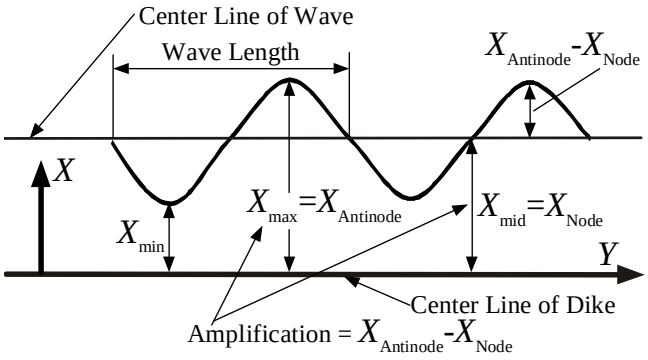

Fig. 6. Definition of wave appears at the top crest of embankment

Results of Series 1 tests

Figure 7 shows the relationships between the frequency of vibration and the normalized amplitude of a nodal point X_{Node} in the Series 1. From this figure it can be seen that the amplitude of a nodal point becomes to a peak state at 14 Hz, and gradient of slope does not influence to the normalized amplitude of the nodal point. Here the predominant frequency is defined as the frequency with the largest amplitude.

Figure 8 shows the relationship between the frequency of vibration and the ratio l/H. From this figure, it can be determined that the ratio in the Series 1-2, Series 1-3 and Serie1-4 is approximately the same, but the ratio in the Series 1-1 is smaller

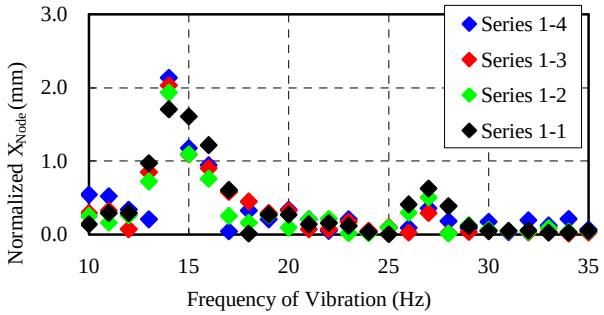

Fig. 7. The relationship between the frequency of vibration and normalized amplitude of a nodal point in Series 1

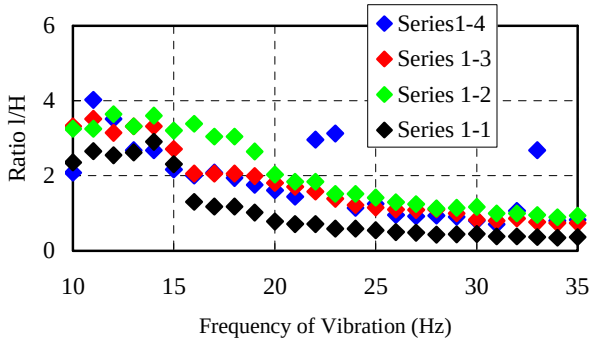

Fig. 8. The relationship between the frequency of vibration and the ratio l/H

than in the others. One can also see that the higher the frequency, the shorter the wavelength becomes..

Results of Series 2 tests

Figure 9 shows the relationship between the frequency of vibration and normalized amplitude of the nodal point X_{Node} in the Series 2. It can be seen from this figure that predominant frequency varies with the shear modulus of embankment and a normalized amplitude of nodal point in the Series 2-1 reaches to 6mm.

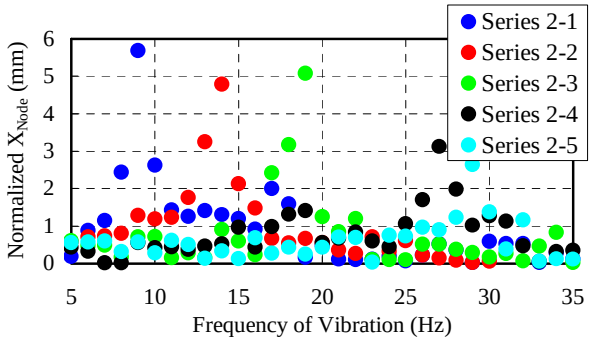

Fig. 9. The relationship between the frequency of vibration and normalized amplitude of a nodal point in Series 2

The relationship between a frequency of vibration and the ratio l/H is plotted in Fig. 10. According to this figure, the wave becomes longer at the high frequency when the model stiffness increases.

Figure 11 shows the relationship between a shear modulus of model embankment and predominant frequency. The predominant frequency becomes higher when the embankment becomes stiffer.

Figure 12 shows the relationship between the shear modulus of

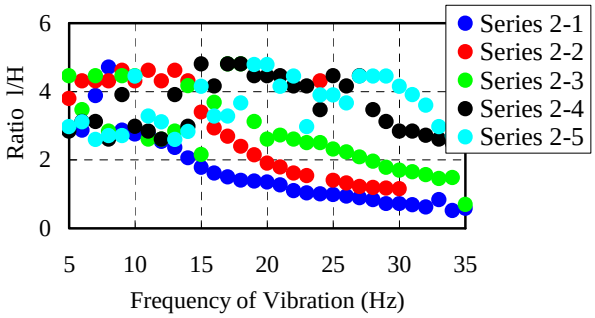

Fig. 10. The relationship between the frequency of vibration and the ratio l/H

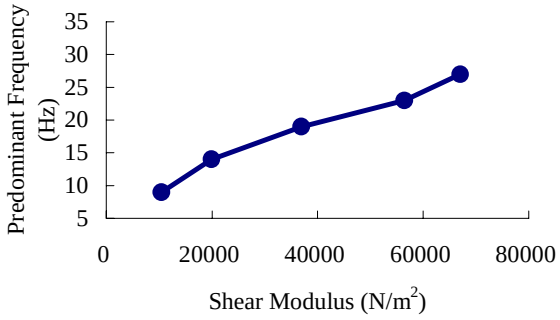

Fig.11. The relationship between the shear modulus of model embankment and predominant frequency

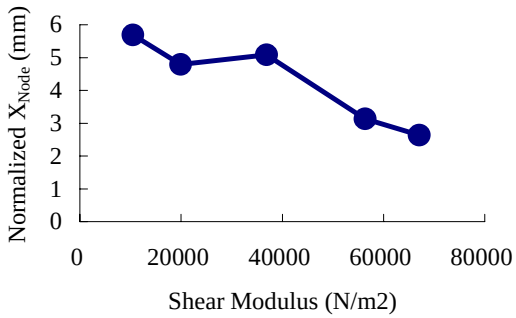

Fig.12. The relationship between the shear modulus of model embankment and the normalized amplitude of a nodal point

model embankment and the normalized amplitude of a nodal point X_{Node} at the first peak. It is found from this figure that the normalized amplitude becomes smaller as the embankment becomes stiffer.

Figure 13 shows the relationship between the shear modulus and a ratio l/H at the resonate frequency. It is clarified that the ratio is independent from the shear modulus of model embankment.

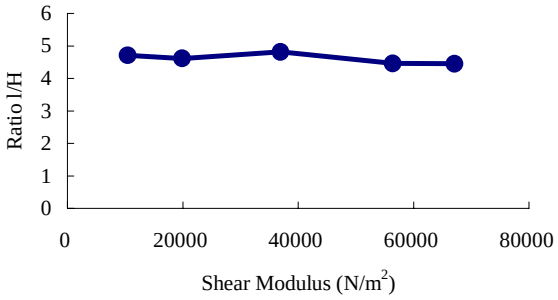

Fig.13. The relationship between the shear modulus of model embankment and the normalized amplitude of a nodal point

Results of Series 3 tests

Figure 14 shows the relationships between the frequency of vibration and normalized amplitude of the nodal point X_{Node} in the Series 3. To compare with the case of 480 mm length, Result of Series 2-2 was plotted together. It is found from this that predominant frequency of Series 3-3 is the same as Series 2-2. However in Series 3-1 and 3-2, predominant frequency becomes higher as the length of embankment becomes shorter. This means that when the length of embankment is long enough, nine times as long as its height, predominant frequency is considered to be constant.

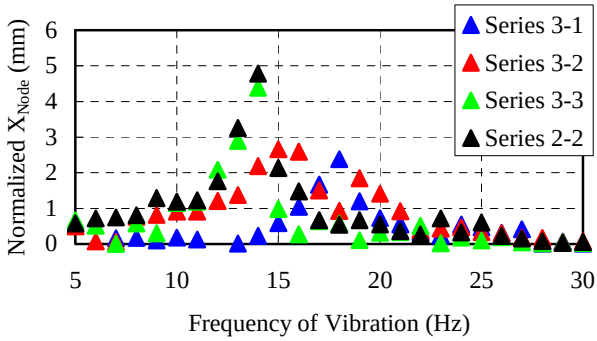

Fig.14. The relationship between the shear modulus of model embankment and the normalized amplitude of a nodal point

Figure 15 shows the relationship between the frequency of vibration and the ratio l/H in Series 3. The ratio (Wavelength /height of embankment) of Series 3-3 is same as one of Series 2-2 But the ratio of Series 3-3 and Series2-2 are slightly smaller than the one of Series 3-1 and 3-2.

From the results of these tests, the following conclusion can be made. The interval of sections where a large response was observed

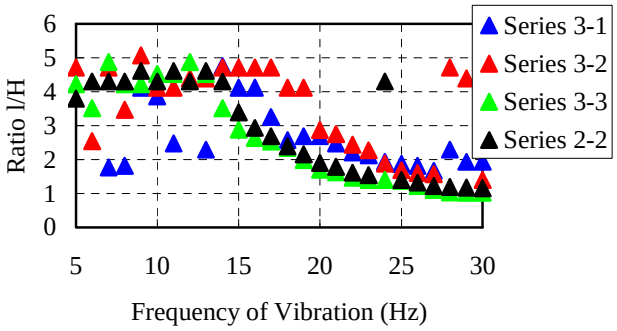

Fig.15. The relationship between the shear modulus of model embankment and the normalized amplitude of a nodal point

depends on the shear rigidity, the length of model and the frequency of the input motion.

COMPARISON OF TESTS RESULTS WITH A THEORETICAL SOLUTION

Ohmachi and Tokimatsu (Ohmachi and Tokimatsu, 1983) reported about a three-dimensional behavior of fill dams during an earthquake, and an equation for vibration shape along the longitudinal axis was derived as follows:

$$\frac{2\pi f_{mn} \cdot H}{V_s} = \sqrt{{\mu_m}^2 + \frac{n^2\pi^2H^2}{L^2}} \,. \qquad (2)$$

Here f_{mn} is the frequency at mth-degree along the height direction and nth-degree along the longitudinal direction. V_s is the shear wave velocity, μ_m is the value of mth-degree which satisfies Bessel function $J_0(\mu_m) = 0$, and L is the length of the dike. The wavelength l is calculated geometrically as follows:

$$l = \frac{2L}{n} \,. \qquad (3)$$

If one substitutes Equation (3) into Equation (2), the next equation related to the wavelength at each frequency along the longitudinal direction can be obtain:

$$l = \frac{2\pi HV_s}{\sqrt{4\pi^2 {f_{mn}}^2 H^2 - {\mu_m}^2 {V_s}^2}} \,. \qquad (4)$$

Figure 16 shows the relationship between the frequency of vibration and the ratio l/H of a theoretical solution derived from Equation (4) for model tests. According to these figures, theoretical solutions of Equation (4) are in good agreement with the test results. Thus, it is possible to calculate the wavelength which appears at the crest of an embankment.

Here l, the wavelength, is real number. It means that the denominator of right side of Equation (4) must be a rational number. Hence, Equation (5) should be satisfied:

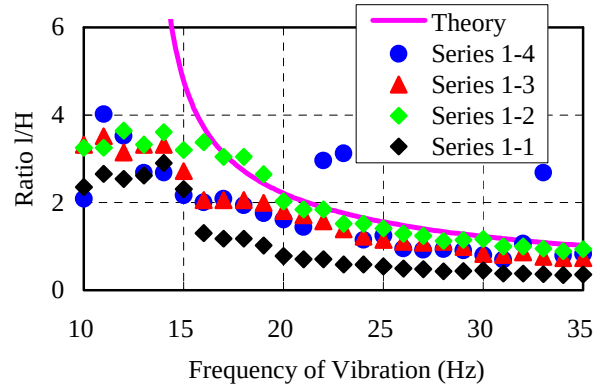

(A) Series 1

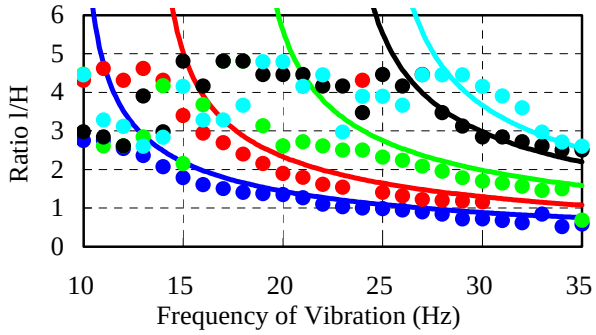

(B) Series 2

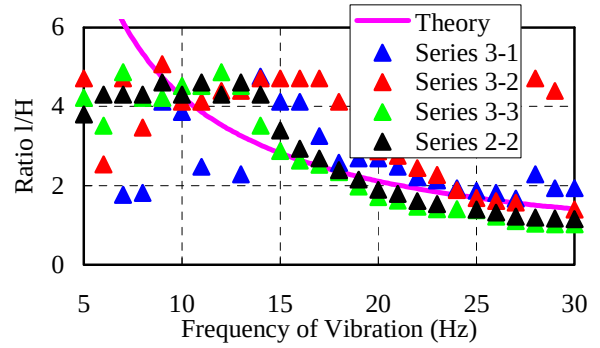

(C) Series 3

Fig.16. The relationship between the frequency of vibration and the ratio l/H of the theoretical solution

$$4\pi^2 f_{mn}{}^2 H^2 - \mu_m{}^2 V_s{}^2 \geq 0 \tag{5}$$

$$\Leftrightarrow f_{mn}{}^2 \geq \frac{\mu_m{}^2 V_s{}^2}{4\pi^2 H^2} \tag{6}$$

$$\Leftrightarrow f_{mn} \geq \sqrt{\frac{\mu_m{}^2 V_s{}^2}{4\pi^2 H^2}} = \frac{\mu_m V_s}{2\pi H} \left(f_{mn} > 0\right). \tag{7}$$

From the shear wave velocity and height of embankment, fundamental frequency of embankment that is calculated as follows:

$$f = \frac{V_s}{4H} = \frac{1}{T}. \tag{8}$$

Substituting Equation (8) into Equation (9), the next equation is obtained:

$$\Leftrightarrow f_{mn} \geq \frac{2\mu_m}{\pi} \approx 1.53 f. \tag{9}$$

In Equation (9), the wave at the crest of an embankment appears only at the frequency which is larger than 1.5 times of the fundamental frequency.

APPLICATION OF THE PROPOSED EQUATION TO IN-SITU DAMAGE OF THE KUSHIRO RIVER DIKE

As shown in Fig. 1, the height of Kushiro River dike is about 6.2 m. The thickness of peat layer under the dike is about 3.3m and one of next loose sandy layer is 3.5 m. According to the in-situ investigation, the shear wave velocity of above two layers is 110 m/s, and one of third layer is 150 m/s. The period of local failure at the top is about 300 m.

Here Equation (4) is derived for the embankment lies on the stiff ground. However, if the shear wave velocity of the soft foundation ground is close to that of the embankment, the ground and the embankment moves simultaneously. Thus, it is possible to calculate the wavelength from Equation (4) using the mean velocity $\overline{V_s}$ of total layer, which is calculated by next equation:

$$\overline{V_s} = \frac{\sum H_i \times V_{si}}{\sum H_i}, \tag{10}$$

where H_i is the height, and V_{si} is the shear wave velocity of i layer.

Unfortunately, there is no earthquake record near the Kushiro dike. However, the site specific ground motion was calculated from the records 1993 Kushiro-Oki earthquake motion by Jiban Kougaku Kenkyusho (JKK,1995), as shown in Fig,. 17. Figure 18 shows the Fourier spectrum of the developed record. From this figure, the

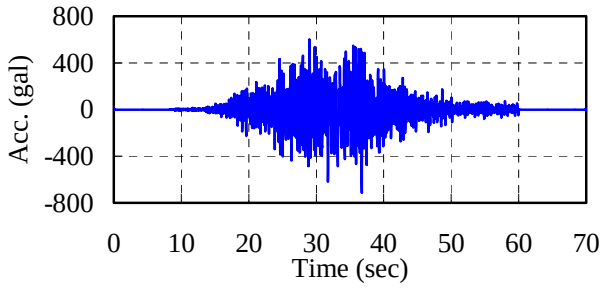

Fig. 17. Site specific ground motion at the Kushiro river dike

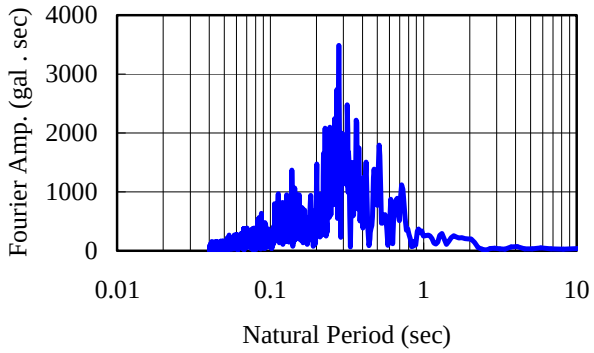

Fig.18. Fourier spectrum of the calculated record

specific frequency ranges from 2 to 5 Hz (0.2 to 0.5 seconds). Figure 19 shows the relationships between wavelength calculated using Equation (4) or (10) and the velocity under 2 to 10 Hz (0.1 to 0.5 seconds). Te interval distance of local failure of the Kushiro River dike was also plotted in these figures as well. It is found from Fig. 19 that the period of the Kushiro River dike can be determined by assuming that the soft layer underneath is accompanied with the embankment.

CONCLUSION

This paper aims to clarify the three-dimensional behavior of embankments during the earthquake. It was found that the local failure of a dike along the longitudinal direction is caused by three-dimensional response of an embankment. After performing the shaking table tests, the interval of sections where a large response was observed depends on the shear rigidity, the length of model and the frequency of the input motion. It was shown that the period of local failure of the embankment during the 1993 Kushiro-Oki Earthquake can be calculated. It was also found that a local failure occurs only when the frequency of shaking is higher than the fundamental frequency of an embankment. Therefore, it is necessary to consider the behavior at other frequency in order to predict seismic design.

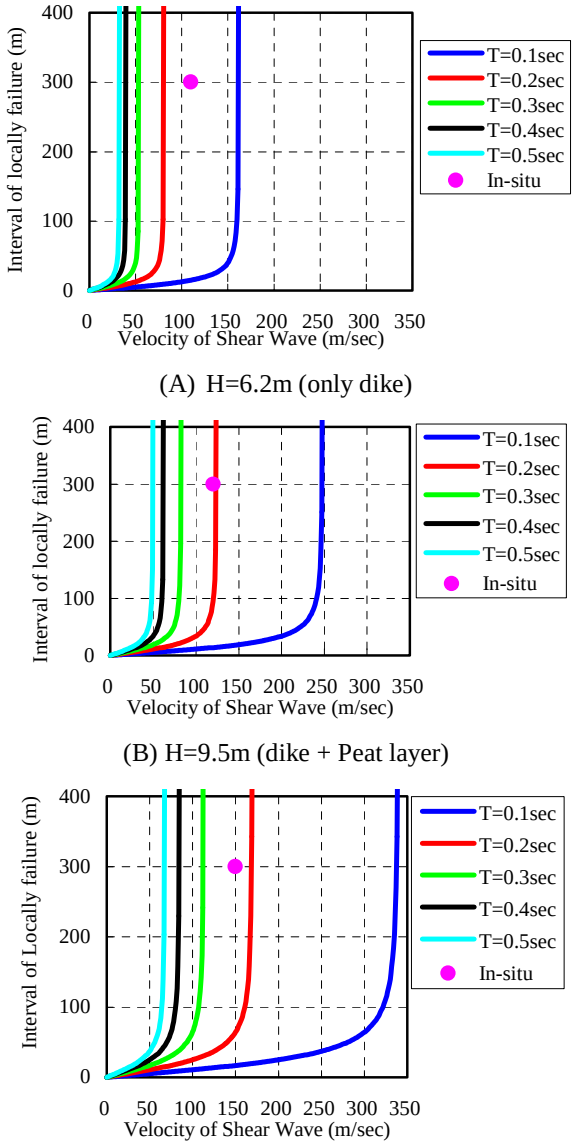

Fig.19. Relationships between the interval of local failure which is calculated with Equation (4) or (10) and the shear wave velocity

REFERENCE

Jiban Kougaku Kenkyusho[1995], Used to refer to date supplied by JKK.

Ohmachi, T. and Tokimatsu, K.[1983], "Formulation of a practical method for three dimensional earthquake response analysis of embankment dams", Proceedings of the Japan Society of Civil Engineering, No.333, pp.71-80 (In Japanese).